Article

Equilibrium and Non-equilibrium Kinetics of Self-Assembled Surfactant Monolayers: A Vibrational Sum-Frequency Study of Dodecanoate at the Fluorite#Water Interface

Simon Schrödle, and Geraldine L. Richmond

J. Am. Chem. Soc., **2008**, 130 (15), 5072-5085 • DOI: 10.1021/ja076664r • Publication Date (Web): 20 March 2008

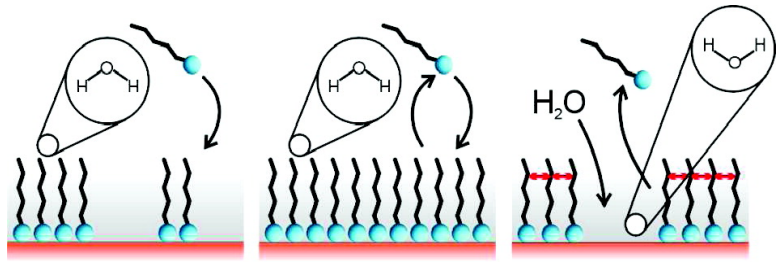

More About This Article

Additional resources and features associated with this article are available within the HTML version:

- Supporting Information
- Links to the 1 articles that cite this article, as of the time of this article download
- Access to high resolution figures
- Links to articles and content related to this article
- Copyright permission to reproduce figures and/or text from this article

View the Full Text HTML

J|A|C|S
ARTICLES

Published on Web 03/20/2008

Equilibrium and Non-equilibrium Kinetics of Self-Assembled Surfactant Monolayers: A Vibrational Sum-Frequency Study of Dodecanoate at the Fluorite−Water Interface

Simon Schrödle and Geraldine L. Richmond*

Department of Chemistry, University of Oregon, Eugene, Oregon 97403-1253

Received September 4, 2007; E-mail: richmond@uoregon.edu

Abstract: The adsorption, desorption, and equilibrium monomer exchange processes of sodium dodecanoate at the fluorite(CaF_2)−water interface have been studied. For the first time, we use in situ vibrational sum-frequency spectroscopy (VSFS) to gain insights into the mechanism and kinetics of monolayer self-assembly at the mineral−water interface. By exploiting the nonlinear optical response of the adsorbate, the temporal correlation of headgroup adsorption and alignment of the surfactant's alkyl chain was monitored. Because of the unique surface-specificity of VSFS, changes in the interfacial water structure were also tracked experimentally. The spectra clearly reveal that the structure of interfacial water molecules is severely disturbed at the start of the adsorption process. With the formation of a well-ordered adsorbate layer, it is partially reestablished; however, the molecular orientation and state of coordination is significantly altered. Even at very low surfactant concentrations, overcharging of the mineral surface (i.e., the adsorption of adsorbates past the point of electrostatic equilibrium) was observed. This points out the importance of effects other than electrostatic interactions and it is proposed that cooperative effects of both water structure and surfactant hemimicelle formation at the interface are key factors. The present study also investigates desorption kinetics of partially and fully established monolayers and a statistical model for data analysis is proposed. Additional experiments were performed in the presence of electrolytes and showed that uni- and divalent anions affect the nonequilibrium kinetics of self-assembled monolayers in strikingly different ways.

1. Introduction

Surfactant adsorption at the solid–liquid interface has many implications for petroleum recovery, mineral separation, and waste management and has thus been subject to intense study.[1–5] In particular, self-assembled adsorbate layers control wetting behavior and reactions at solid substrates and govern stability and rheology of suspensions. Compared to aggregation in bulk phases,[6] adsorption at solid–liquid interfaces exhibits quite slow kinetics.[7] Therefore, nonequilibrium adsorption states[8] are frequently present, as processes at phase boundaries often operate—for economic reasons or because of a constant variation of bulk composition—far from equilibrium and are determined by mass transport or rate-limiting surface reactions.[9] Understanding of these complex systems thus requires detailed knowledge of the molecular exchange processes between interfacial layer and bulk, which govern their behavior. Unfortunately, such studies are rare[10–14] and still pose severe problems for the experimentalist, especially at buried interfaces.[15] The available literature focuses mainly on the adsorbate–substrate interaction or only reports thermodynamic (surface excess) data. Moreover, information on the temporal evolution of interfacial water structure during the adsorption process is lacking, as most commonly employed methods based on infrared (IR) spectroscopy[16–18] are not inherently surface-sensitive but rather probe a layer which can be up to several μm in thickness. The analysis of such spectroscopic data is additionally complicated by congested spectra, which make the separation of interfacial from bulk species impracticable. This is especially true for the spectral response of water, which generally is predominant in the 2600−4000 cm^{-1} region. The underlaying OH resonances are characterized by large line width and amplitude, thus preventing

(1) Sharma, R. *Surfactant Adsorption and Surface Solubilization*; American Chemical Society: Washington, DC, 1995.
(2) Sparks, D. L. *J. Plant Nutr. Soil Sci.* **2000**, *163*, 563–570.
(3) Parekh, B. K.; Miller, J. D. *Advances in flotation technology*; Society for Mining, Metallurgy, and Exploration, Inc. (SME): Littleton, CO, 1999.
(4) Fenter, P.; Sturchio, N. C. *Prog. Surf. Sci.* **2004**, *77*, 171–258.
(5) Hopkins, A. J.; McFaerin, C. L.; Richmond, G. L. *Curr. Opin. Solid State Mater. Sci.* **2005**, *9*, 19–27.
(6) Aniansson, E. A. G.; Wall, S. N.; Almgren, M.; Hoffmann, H.; Kielmann, I.; Ulbricht, W.; Zana, R.; Lang, J.; Tondre, C. *J. Phys. Chem.* **1976**, *80*, 905–922.
(7) Clark, S. C.; Ducker, W. A. *J. Phys. Chem. B* **2003**, *107*, 9011–9021.
(8) Fuerstenau, D. W. *J. Colloid Interface Sci.* **2002**, *256*, 79–90.
(9) Dukhin, S. S.; Kretzschmar, G.; Miller, R. *Dynamics of Adsorption at Liquid Interfaces*; Elsevier: Amsterdam, The Netherlands, 1995.
(10) Couzis, A.; Gulari, E. *Langmuir* **1993**, *9*, 3414–3421.
(11) Free, M. L.; Miller, J. D. *Langmuir* **1997**, *13*, 4377–4382.
(12) Mielczarski, J. A.; Mielczarski, E.; Cases, J. M. *Langmuir* **1999**, *15*, 500–508.
(13) Li, H.; Tripp, C. P. *Langmuir* **2002**, *18*, 9441–9446.
(14) Atkin, R.; Craig, V. S. J.; Wanless, E. J.; Biggs, S. *J. Colloid Interface Sci.* **2003**, *266*, 236–244.
(15) Atkin, R.; Craig, V. S. J.; Wanless, E. J.; Biggs, S. *Adv. Colloid Interface Sci.* **2003**, *103*, 219–304.
(16) Young, C. A.; Miller, J. D. *Miner. Metal. Process.* **2001**, *18*, 38–44.
(17) Lu, Y.; Miller, J. D. *J. Colloid Interface Sci.* **2002**, *256*, 41–52.
(18) Mielczarski, E.; Mielczarski, J. A. *C. R. Geoscience* **2002**, *334*, 703–715.

10.1021/ja076664r CCC: $40.75

a decomposition of linear IR spectra into contributions from interfacial and bulk water species.

The more recently introduced vibrational sum-frequency spectroscopy (VSFS) exploits the inherent surface specificity of a nonlinear optical effect and has already provided tremendous insight into adsorption and molecular orientation at interfaces.[5] Virtually all of these studies are, however, limited to static systems. With advances in optical engineering, pulsed laser sources became available that allow rapid tuning within a broad range of wavenumbers and which provide stable operation for hours, or even days. Thus, vibrational modes corresponding to different molecules, or distinct groups of a molecule, can be probed almost simultaneously, and their intensity can be recorded as a function of time and related to molecular processes.[19,20]

The fluorite−water interface provides a good model system for studying the kinetics of adsorption at a solid–liquid interface. Previous studies from this laboratory[21–23] have laid the groundwork for those time-dependent measurements. Fluorite (CaF_2) itself is an important industrial mineral and generally separated from unwanted (gangue) materials by froth flotation.[11] Additionally it represents a typical example of a semisoluble ionic substrate. From previous studies, it is known that the CaF_2 surface is fluoride deficient because of preferential solvation of the F^- ion in water.[24,25] The main surface species of hydrated fluorite other than Ca^{2+} and F^- are hydroxyl groups.[26] Therefore, the fluorite surface in contact with water can resemble the solid-water interface of a variety of calcium minerals (e.g., calcite, apatite, wollastonite)[27] of high technological significance and environmental abundance.[28]

It has long been known that fluorite exhibits, at acid and neutral pH in the absence of surface carbonation, a high positive surface potential.[29,30] Only at high pH values of the bulk liquid in contact with CaF_2 (pH $\geq$ 9), does negative charging occur. The positive surface attracts anions toward the interface, which can either be located in an adsorbate layer close to the surface or present in more randomly ordered fashion.[31,32] For this study, dodecanoate was chosen as the adsorbate because it allows the investigation of adsorption and desorption on experimentally favorable timescales (hours). On the contrary, long-chain carboxylates[23] exhibit extremely slow kinetics and an equilibrium situation may not be achieved even after days. Moreover, desorption of such layers, which build up to a considerable hydrophobic barrier at the fluorite surface, is likely to be kinetically inhibited or at least too slow for the capabilities of the present technique. Dodecanoate thus occupies an intermediate position between long-chain carboxylates forming particularly well-ordered layers which may show experimentally nonpractical kinetics and short-chain carboxylates where interactions between the alkyl chains are weak.[31] The discrete headgroup−substrate interaction for dodecanoate, however, is arguably very similar to its lower and higher homologues.

To our knowledge, dodecanoate (C_{12}) adsorption at the fluorite−water interface has been previously studied by VSFS only in the 1400−1500 cm^{-1} range.[31] A band centered at ~1450 cm^{-1} was observed and ascribed to a carboxylate headgroup band, with contributions from several local modes. At higher frequencies (2800−3800 cm^{-1}) additional spectral features can be expected, which should resemble those of other long-chain carboxylates, for example, decanoate (C_{10}) or stearate (C_{18}).[23] In short, strong bands from CH_3 groups were reported for stearate at 2872 and 2932 cm^{-1} respectively,[23] and assigned to a symmetric stretch and a CH_3 bending overtone. The latter is enhanced by Fermi resonance.

Signatures of interfacial water molecules are typically found at ~3200 cm^{-1} and ~3450 cm^{-1} in the VSFS spectra, arising from OH oscillators in highly (tetrahedrally) ordered and more asymmetrically linked hydrogen-bond environments, respectively.[21]

In contrast to the VSFS spectra of neat water at a number of solid–liquid interfaces,[33,21,34,35] little is known about the effect of electrolytes on the structuring of water near such interfaces. Most of the previous work has been done using electrokinetic methods,[25] and very few detailed studies related to the effect of electrolytes, and ionic strength in general, on surfactant adsorption kinetics at surfaces of semisoluble minerals are available.[11] As many aqueous systems contain a considerable quantity of ions, the present investigation also presents a first account of a nonlinear spectroscopic study of electrolytes at the fluorite−water interface and their effect on adsorption, desorption, and equilibrium exchange kinetics.

2. Background

Comprehensive reviews of VSFS theory[36,37] have been given elsewhere and only the essentials need to be repeated here.

For the current experiments, two short laser pulses, one with fixed frequency ω_{VIS} in the visible and the other tunable in the IR range (ω_{VIR}), are spatially and temporally overlapped at the interface. The wavelength of the visible beam is chosen to be off resonance, thus, the interfacial second-order nonlinear susceptibility $\chi^{(2)}$ only depends on the IR frequency, and measured sum frequency spectra are of the form

$$I_{SF}(\omega_{IR}) \propto |\chi^{(2)}|^2 I_{VIS} I_{IR} L_{SFG}^2 L_{VIS}^2 L_{IR}^2 \quad (1)$$

In eq 1, I_{VIS} and I_{IS} denote the intensities of the incident beams, and the L terms are the Fresnel factors.

$\chi^{(2)}$, which is proportional to the square root of the sum-frequency intensity normalized by the power of the incident

(19) Liu, J.; Conboy, J. C. *J. Am. Chem. Soc.* **2004**, *126*, 8376–8377.
(20) Anglin, T. C.; Liu, J.; Conboy, J. C. *Biophys. J.* **2007**, *92*, L01–L03.
(21) Becraft, K. A.; Richmond, G. L. *Langmuir* **2001**, *17*, 7721–7724.
(22) Becraft, K. A.; Moore, F. G.; Richmond, G. L. *J. Phys. Chem. B* **2003**, *107*, 3675–3678.
(23) Becraft, K. A.; Richmond, G. L. *J. Phys. Chem. B* **2005**, *109*, 5108–5117.
(24) Veeramasuneni, S.; Hu, Y.; Miller, J. D. *Surf. Sci.* **1997**, *382*, 127–136.
(25) Hu, Y.; Lu, Y.; Veeramasuneni, S.; Miller, J. D. *J. Colloid Interface Sci.* **1997**, *190*, 224–231.
(26) Wu, L.; Forsling, W. *J. Colloid Interface Sci.* **1995**, *174*, 178–184.
(27) Wu, L.; Forsling, W.; Schindler, P. W. *J. Colloid Interface Sci.* **1991**, *147*, 178–185.
(28) Holmgren, A.; Wu, L.; Forsling, W. *Spectrochim. Acta, Part A* **1994**, *50A*, 1857–1869.
(29) Miller, J. D.; Hiskey, J. B. *J. Colloid Interface Sci.* **1972**, *41*, 567–573.
(30) Miller, J. D.; Fa, K.; Calara, J. V.; Paruchuri, V. K. *Colloids Surf., A* **2004**, *238*, 91–97.
(31) Schrödle, S.; Moore, F. G.; Richmond, G. L. *J. Phys. Chem. C* **2007**, *111*, 8050–8059.
(32) Schrödle, S.; Moore, F. G.; Richmond, G. L. *J. Phys. Chem. C* **2007**, *111*, 10088–10094.
(33) Yaganeh, M. S.; Dougal, S. M.; Pink, H. S. *Phys. Rev. Lett.* **1999**, *83*, 1179–1182.
(34) Kataoka, S.; Gurau, M. C.; Albertorio, F.; Holden, M. A.; Lim, S.-M.; Yang, R. D.; Cremer, P. S. *Langmuir* **2004**, *20*, 1662–1666.
(35) Ostroverkhov, V.; Waychunas, G. A.; Shen, Y. R. *Chem. Phys. Lett.* **2004**, *386*, 144–148.
(36) Shen, Y. R. *The Principles of Nonlinear Optics;* Wiley: New York, 1984.
(37) Richmond, G. L. *Chem. Rev.* **2002**, *102*, 2693–2724.

beams, can be represented by a coherent superposition of a nonresonant part $\chi_{NR}^{(2)}$ and resonant components of the susceptibility, $\chi_{R,i}^{(2)}$ (eq 2).

$$\chi^{(2)} = \chi_{NR}^{(2)} + \sum_i \chi_{R,i}^{(2)} \quad (2)$$

$\chi_{NR}^{(2)}$ is assumed to be real for the CaF_2 interface, but the resonant contributions $\chi_{R,i}^{(2)}$ are complex. The latter arise from the orientational average of the molecular hyperpolarizabilities of the N molecules in the interfacial region:

$$\chi_{R,i}^{(2)} \propto N\langle\beta\rangle \quad (3)$$

The $\chi_{R,i}^{(2)}$ were described by a vibrational response function, convoluted with a Gaussian distribution to incorporate inhomogeneous broadening (eq 4).[23]

$$\chi_{R,i}^{(2)} = A_i e^{i\gamma_i} \int_0^\infty \frac{1}{\omega_{IR} - \omega_L + i\Gamma_L} \times \exp\left[-\frac{(\omega_L - \omega_i)^2}{\Gamma_i^2}\right] d\omega_L \quad (4)$$

In this equation, A_i, γ_i, ω_i and Γ_L are the amplitude, phase, center frequency, and homogeneous (Lorentzian) line width of the ith mode. Γ_i accounts for inhomogeneous broadening. Given the spectral width of the IR beam ($\sim$6 cm^{-1}) and thus $\Gamma_i \gg \Gamma_L$, the peak shape is not sensitive to Γ_L and a constant value $\Gamma_L = 5$ cm^{-1} was used throughout. For the determination of the adsorption isotherm, Γ_i and ω_i were determined from a global fit of the spectra.

For this study, all spectra were obtained using the *ssp* polarization scheme. The letters represent light polarized parallel to the plane of incidence (*p*) or perpendicular to the plane of incidence (*s*) and their order is in decreasing frequency; that is, in the present case sum-frequency and visible probe beams are *s* polarized, while the tunable IR beam is *p* polarized, thus probing the $\chi_{yyz}^{(2)}$ component of the second-order interfacial susceptibility tensor, with the *z* axis normal to the interface, and *xz* as the plane of incidence.

3. Experimental Details

Details of the laser system[32,31] and experimental setup[21] have been reported elsewhere. For the current VSFS experiments, the IR and visible (532 nm) laser pulses (duration $\sim$30 ps, produced by a commercial laser and parametric oscillator/amplifier) were incident on a CaF_2 prism (68°) at near critical angles, 17° and 20.5°, respectively. High-efficiency filters and dispersive optics were used to select the sum-frequency photons which were metered by a photomultiplier.

For the experiments monitoring simultaneous changes in different frequency regions, the VSFS instrument was equipped with a computer-controlled beam steering device. Further details on technical aspects and the experimental protocol can be found elsewhere.[38]

To prevent depletion of the very dilute samples and to avoid effects caused by ions from the semisoluble fluorite substrate, a peristaltic pump was used to constantly flush the prism surface with fresh sample liquid or ultrapure water (desorption experiments).

Sodium dodecanoate (C12-H) was a commercial product of TCI America and samples were prepared by diluting a $\sim$1 mM stock solution. The dissolved surfactant showed noticeable decomposition over the course of a few days. Solutions where thus freshly prepared at the start of each series of experiments (daily). The preparation of sodium dodecanoate-12,12,12-d_3 (C12-D) solutions from dodecanoic acid-12,12,12-d_3 (CDN Isotopes; 99.7% purity, 99.8% deuteration) has been described previously.[39] Acetic acid-d_4 (Aldrich) had a purity and degree of deuteration exceeding 99.5% and was used as received. Sodium acetate, sodium chloride, sodium hydroxide and sodium sulfate were all of ACS certified analytical purity.

The pH of the (only very weakly buffered) solutions was occasionally checked by a calibrated pH meter connected to a glass electrode and found at $\sim 6 \pm 0.5$. All ionic strength values and concentrations are given in M, 1 M = 1 mol L^{-1} .

High purity water obtained from a Barnstead NANOpure II system (resistivity >18 MΩ cm) was used throughout. All glassware was cleaned by prolonged soaking in concentrated sulfuric acid with added ammonium peroxodisulfate and rinsing with copious amounts of purified water.

The CaF_2 prism was regularly polished with 0.05 μm Al_2O_3 powder. At intervals, extensive cleaning was performed by a thorough polish using 3 and 1 μm diamond paste or by soaking in diluted (0.1 M) hydrochloric acid and methanol (HPLC grade). The cleanliness was frequently monitored by recording VSFS spectra of the neat prism−water interface.

4. Results and Discussion

4.1. Monolayer Adsorption Isotherm. Adsorption isotherms, in the thermodynamic sense, describe the relationship between surface excess and bulk concentration. The surface excess is defined as the difference between the amount of surfactant actually present in a system, and that which would be present if the bulk concentrations were maintained up to the dividing surface.[40] As such, it is not specific for the kind of adsorbate–substrate interaction, the orientation and order of surfactant molecules, or the width of the interfacial region where the adsorbate concentration is enhanced. The limitations of macroscopic approaches to measuring the surface excess have long been noted,[41] and (linear) FTIR spectroscopy has since been introduced as a tool for in situ investigations. Consequently, internal reflection IR techniques were developed into quantitative tools for the determination of adsorption isotherms.[10,12,42–47] It was found that these spectroscopic results compare well with thermodynamic adsorption studies, for example, solution depletion experiments.[42] This is advantageous as long as the study of the overall adsorption process is concerned, but shows the low specificity of linear IR techniques for the mesoscopic state of order and aggregation of interfacial molecules. The lack of specificity also caused significant debate about the nature of the adsorbate layer,[3] even for equilibrium adsorption.[17,46,48–50]

(38) Schrödle, S.; Richmond, G. L. *Appl. Spectrosc.* **2008**, in press.
(39) Schrödle, S.; Richmond, G. L. *ChemPhysChem* **2007**, *8*, 2315–2317.
(40) McNaught, A. D.; Wilkinson, A. *Compendium of Chemical Terminology*, 2nd ed.; Blackwell Science: Oxford, U.K., 1997.
(41) Davis, J. A.; Hayes, K. F. *Geochemical Processes at Mineral Surfaces;* American Chemical Society: Washington, DC, 1986.
(42) Sperline, R. P.; Muralidharan, S.; Freiser, H. *Langmuir* **1987**, *3*, 198–202.
(43) Kellar, J. J.; Cross, W. M.; Miller, J. D. *Appl. Spectrosc.* **1989**, *43*, 1456–1459.
(44) Kellar, J. J.; Cross, W. M.; Miller, J. D. *Appl. Spectrosc.* **1990**, *44*, 1508–1512.
(45) Fa, K.; Miller, J. D. *J. Chem. Phys.* **2003**, *119*, 13068–13076.
(46) Mielczarski, J. A.; Mielczarski, E. *J. Phys. Chem.* **1995**, *99*, 3206–3217.
(47) Mielczarski, J. A.; Mielczarski, E. *Phys. Probl. Miner. Proc.* **2005**, *39*, 33–46.
(48) Kellar, J. J.; Cross, W. M.; Miller, J. D. *Sep. Sci. Technol.* **1990**, *25*, 2133–2155.
(49) Mielczarski, J. A.; Casses, J. M.; Bouquet, E.; Barres, O.; Delon, J. F. *Langmuir* **1993**, *9*, 2370–2382.
(50) Miller, J. D.; Jang, W.-H.; Kellar, J. J. *Langmuir* **1995**, *11*, 3272–3274.

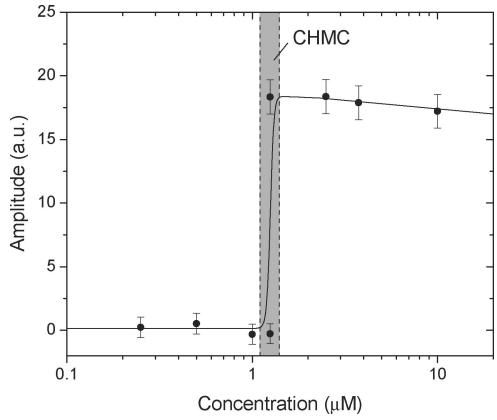

Figure 1. Adsorption isotherm of sodium dodecanoate at the water/CaF_2 interface. Amplitudes were determined from fits of *ssp* polarized spectra (1350–1600 cm^{-1}). Curve is shown as a guide to the eye only.

In principle, polarization-resolved IR spectroscopy can yield data on molecular orientation,[46,51] but has rarely been employed to obtain quantitative or kinetic data.

In 1955, Gaudin and Fuerstenau[52] introduced the notion of a substrate-supported self-assembled monolayer, termed a hemimicelle, and proposed bilayer formation at higher surfactant bulk concentration.[8,52] In analogy the bulk critical micellar concentration (CMC), a critical hemimicellar concentration (CHMC) can be observed[8] For some surfactants, the situation can be complicated by surface precipitation.[3] Additionally, discrete aggregates can be formed at the interface or adsorbed from the bulk.[15] This makes a study of adsorption phenomena using a truly surface-specific experimental technique highly desirable.

Using VSFS, an adsorption isotherm can be determined, which differs from the thermodynamic notion of an isotherm. Because of the orientational specificity of the nonlinear sum-frequency process, only molecules with a net orientation relative to the interface contribute to the spectra. It has been stated before that for the present study, the $\chi_{yyz}^{(2)}$ element of the $\chi^{(2)}$ tensor is probed. The resonant component of this element specifically arises from the orientational average of molecular polarizability contributions perpendicular to the surface. Fortunately, in the region 1400−1500 cm^{-1}, there is only one resonant contribution to the VSFS spectrum, a carboxylate headgroup band.[31,32] Evaluating the amplitude of this band derived from spectral fits (eq 4) as a function of bulk surfactant concentration, one can determine an adsorption isotherm specific for *oriented* surfactant molecules. Figure 1 shows the result of such a study. Note that because of the coherent nature of the sum-frequency process, oppositely oriented surfactant molecules, for example, in a bilayer or admicellar structure, lead to destructive interference and the total amplitude of the signal caused by $\chi_{yyz}^{(2)}$ would be diminished accordingly.[22]

The VSFS isotherm presented in Figure 1 clearly reveals a sharp increase of the amplitude from the carboxylate band at the CHMC (~1.25 μM), which is significantly lower than the CMC[53] (~24 mM). Classical thermodynamic isotherms, which measure the total adsorption density regardless of the molecular environment of the adsorbate, generally show a gradual increase in the surface concentration, with the CHMC often only appearing as a change in the slope. In contrast, the interfacial density of the molecules probed by VSFS undergo a much more dramatic change and as long as depletion of the bulk solution is avoided, virtually identical sum-frequency amplitudes were reached for $c > c_{CHMC}$, indicating the same equilibrium density of oriented molecules at the interface. The thermodynamic surface excess does not necessarily follow the same trend, because the VSFS signal is proportional to both the number of molecules and their net orientation toward the interface. The concentration range around the CHMC corresponding to intermediate oriented surface coverage appears to be very small. Monolayer formation on fluorite is thus a truly critical process driven by highly cooperative adsorption and conformational alignment of monomers. The slight decrease in amplitude above the CHMC (Figure 1) is within the error limits of the experiment, given by the drift of the laser and beam overlap, but could also be evidence for a slightly lower degree of order in monolayers grown from higher surfactant bulk concentrations. From kinetic data (see below), bilayer formation appears to be an unlikely reason, because the measured coverage rises strictly monotonically during adsorption. Carboxylates similar to dodecanoate do not usually form bilayer structures over the concentration range relevant here.[23] Any increase of the thermodynamic surface excess past the CHMC, which would be measurable with classical or linear IR experiments, can therefore be attributed to a concentration enhancement of monomeric, randomly oriented surfactant in the interfacial region.

It has to be stressed again that the current method selectively probes only molecules with a net orientation relative to the interface. Consequently, any diffuse surface excess present below the CHMC, as has often been observed by thermodynamic or FTIR[54] experiments and, obviously, additional adsorption in a diffuse region above the monolayer for $c > c_{CHMC}$, does not interfere with the experiment. This sensitivity and selectivity advantage of VSFS clearly shows that a well-defined transition from a disordered state of the interfacial region to a highly aligned layer occurs at ~1.25 μM. Below the CHMC, the thermodynamic surface excess of the surfactant may already be notable, but molecules are only present in a sum-frequency inactive state; that is, they are not incorporated into mesoscopically organized structures.[55] The same applies to molecules adsorbed beyond the surface layer above the CHMC, which are unlikely to show strong net orientation relative to the interface as long as they are not organized in a layered structure because of the high conformational freedom of the alkyl chain of isolated monomers.

4.2. Charge Reversal: Using Water as a Molecular Probe. In addition to the headgroup response, the wide-band tunability of the VSFS system employed for this study offers an opportunity to study the methyl and methylene response of adsorbed dodecanoate molecules as well as the interfacial water structure, similar to earlier work on related surfactants.[23] Two spectra were recorded corresponding to a surface at partial or full equilibrium coverage, Figure 2 and Figure 3, respectively. Spectral decompositions are shown in Figures 2a and 3a. Bands attributed to the adsorbate monolayer (red) are located at 2728, 2874, and 2933 cm^{-1}, blue curves indicate the contributions from interfacial water molecules (~3200 cm^{-1} and ~3450 cm^{-1}).[21] Additionally, the phase relationship of the peaks is

(51) Neivandt, D. J.; Gee, M. L.; Hair, M. L.; Tripp, C. P. *J. Phys. Chem. B* **1998**, *102*, 5107–5114.
(52) Gaudin, A. M.; Fuerstenau, D. W. *Trans. AIME* **1955**, *202*, 958–962.
(53) Mukerjee, P.; Mysels, K. J. *Natl. Stand. Ref. Data Ser.* **1971**, *36*, 137.
(54) Jang, W. H.; Miller, J. D. *Langmuir* **1993**, *9*, 3159–3165.
(55) Somasundaran, P.; Kunjappu, J. T. *Miner. Metal. Process.* **1988**, *5*, 68–79.

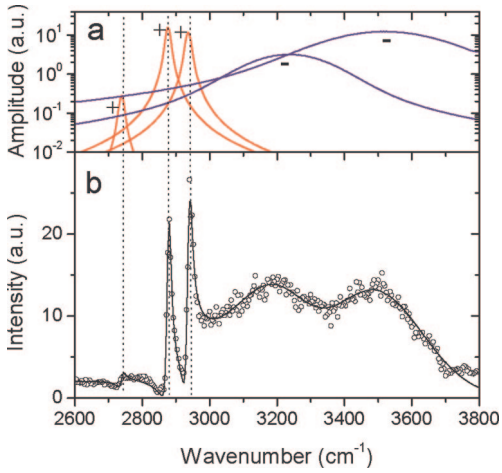

Figure 2. Decomposition (a) of VSFS spectra (b) of the sodium dodecanoate(aq)/CaF_2 interface at ~30% saturation coverage. Signs indicate the relative phases of the signals. Red curves represent adsorbate contributions, blue peaks are attributed to water modes (see text).

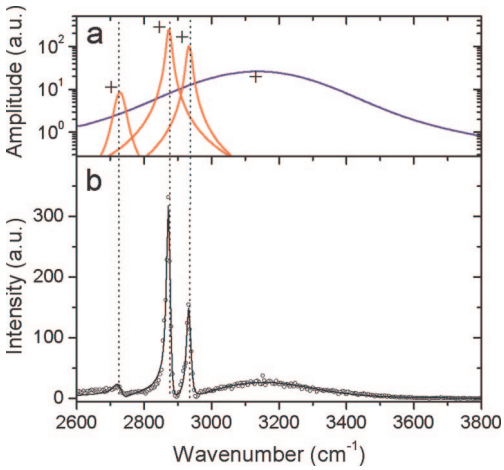

Figure 3. Decomposition (a) of VSFS spectra (b) of the sodium dodecanoate (aq)/CaF_2 interface at complete coverage.[39] Signs indicate the relative phases of the signals. Red curves represent adsorbate contributions, blue peaks are attributed to water modes (see text).

indicated by signs: at low coverage, the susceptibility contributions of surfactant and water have opposite signs (destructive interference), at full coverage, all peaks are interfering constructively. This change in the phase of the signals arises from a flip of the preferential orientation of interfacial water molecules[22,23,56] and thus provides a sensitive means to probe the electric field close to the adsorbate layer. For the neat CaF_2–water interface, fluorite is positively charged, orienting water molecules with their oxygen atoms pointing toward the surface.[21] At a later point, continued adsorption and build-up of the monolayer leads to overcharging of the surface (see below), and the orientation of the water molecules is reversed with respect to the interface.

Figures 2 and 3 also reveal another interesting aspect of the adsorption process: changes in the relative abundance of water molecules in a highly symmetrically coordinated environment, referred to here as tetrahedral (at ~3200 cm^{-1}) or a more disordered (at ~3450 cm^{-1}) state. While the former is the highly predominant species at the neat fluorite–water interface,[21,31] the ratio shifts significantly with preceding dodecanoate adsorption. Clearly, in Figure 2, the amplitude of disordered interfacial water molecules is considerably higher than that of the tetrahedrally bonded species. A similar redistribution can be observed for acetate adsorption at the CaF_2–water interface[31] and seems to be connected with the presence of adsorbate molecules close to the surface. Such ions reduce the number of water molecules which are exposed to an orienting surface field, but still not in the vicinity of an ion, which would disturb the symmetrical hydrogen-bond coordination prerequisite for the ~3200 cm^{-1} response.

After charge reversal, the band at 3450 cm^{-1} has vanished (Figure 3). This indicates strong, symmetric structuring of water molecules near the now hydrophobic interface, and the orienting surface field does not extend far enough into more disordered water regions adjacent to the monolayer to generate a detectable VSFS response.

4.3. Temporal Evolution of the Interface. It has already been noted that the present understanding of adsorption at the mineral–water interfaces is still largely based on thermodynamic measurements, such as adsorption isotherms and (to a lesser extent) adsorption kinetics, that is, the measurement of surface excess concentrations as a function of time.[11,13,51,57–62] These data are then usually interpreted in terms of the microscopic structure of the interface.[1] Specific substrate–adsorbate interactions and other effects (ion–ion correlation, hydrophobic interactions, complex formation at the interface) are frequently incorporated in models to characterize the equilibrium adsorption state.[63] The inherent dangers of these quite common approaches have been stated by various investigators.[15,64] Thermodynamic properties in general are not specific to the microstructure of the interface, and in particular, mechanistic aspects of the adsorption process can hardly be inferred from thermodynamic data of adsorbate layers in their equilibrium state. Thermodynamics can accommodate various interfacial models as long as the surface excess meets the requirements of the Gibbs equation.

Even more important, the role of the solvent (and in particular, of water) for interfacial processes has long been recognized,[9,15] but its investigation remains a difficult experimental task. Of the few techniques capable of studying interfacial water structure, VSFS has already revealed substantial detail of water orientation at the fluorite–water interface in the presence of various organic adsorbates.[23,31,32] Despite these advances in recent times, with equilibrated surfaces, a more comprehensive understanding of adsorption processes requires information on the molecular pathways: the synchronization of substrate–adsorbate bonding with changes in water structure, conformational alignment of the adsorbate layer,[65] the coordination state of interfacial water molecules,[21] and the distribution of ions at the interface, which determine the intricate electrostatic balance at the solid-water contact.[63]

(56) Becraft, K. A.; Moore, F. G.; Richmond, G. L. *Phys. Chem. Chem. Phys.* **2004**, *6*, 1880–1889.
(57) Malbrel, C. A.; Somasundaran, P.; Turro, N. J. *J. Colloid Interface Sci.* **1990**, *137*, 600–603.
(58) Tiberg, F.; Jönsson, B.; Lindman, B. *Langmuir* **1994**, *10*, 3714–3722.
(59) Atkin, R.; Craig, V. S. J.; Biggs, S. *Langmuir* **2001**, *17*, 6155–6163.
(60) Pagac, E. S.; Prieve, D. C.; Tilton, R. D. *Langmuir* **1998**, *14*, 2333–2342.
(61) Velegol, S. B.; Fleming, B. D.; Biggs, S.; Wanless, E. J.; Tilton, R. D. *Langmuir* **2000**, *16*, 2548–2556.
(62) Biswas, S. C.; Chattoraj, D. K. *J. Colloid Surface Sci.* **1998**, *205*, 12–20.
(63) Lyklema, J. *Colloids Surf., A* **2006**, *291*, 3–12.
(64) Sposito, G. *J. Colloid Interface Sci.* **1983**, *91*, 329–340.
(65) Holland, P. *ACS Symp. Ser.* **1992**,*501,* 354–365..

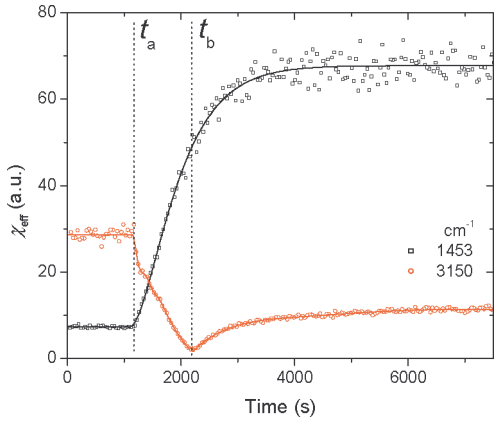

Figure 4. Temporal evolution of sum-frequency signals at 1453 (black) and 3150 cm^{-1} (red), corresponding to the response of the carboxylate headgroup and ordered water molecules, respectively. At time t_a, the concentration of sodium dodecanoate in the aqueous phase was increased from 0 to 5 μM. A minimum of the water response is observed at t_b.

The VSFS signatures of the carboxylate headgroup and the H-bonded water molecules are located in quite different wavenumber regions of the sum-frequency spectrum and thus, exploiting the advantages of a wide-band, rapidly tunable IR source and sum-frequency detection system, the evolution of the sum-frequency signal can be followed virtually simultaneously at different frequencies characteristic of specific molecular subunits within the interfacial layer. This is done by sequentially changing the setup parameters of the OPO/OPA/DFG system every 15 s.[38] For this study, 1453 cm^{-1} and 3150 cm^{-1} were chosen to monitor the intensities of the carboxylate headgroup and water bands, respectively.

Figure 4 presents results for the adsorption process, following an increase of dodecanoate concentration from neat water to 5 μM. At the time of concentration change (t_a), the amplitude of the water response is immediately diminished by ~30%, followed by a slower decrease. This indicates that the number of tetrahedrally coordinated water molecules at the interface dramatically decreases in the presence of even minute amounts of surfactant in a near-surface layer, well before a monolayer is formed. Note that this is not just an effect of the slightly increased ionic strength of the bulk medium containing surfactant compared to neat water, because the ionic strength of nonadsorbing, monovalent electrolytes has no measurable effect on the water amplitudes at micromolar concentrations (see later). Thus, surfactant molecules, albeit not yet ordered or adsorbed directly at the interface, considerably affect the hydrogen-bonding environment close to the CaF_2 surface.

Following this immediate response, monolayer assembly at the interface ensues. At t_b (Figure 4), the signal caused by oriented water molecules reaches a minimum, hardly above the nonresonant background signal of a neat CaF_2−water interface. Notice that at this point, the surface coverage measured by the headgroup signal at 1453 cm^{-1} is far from equilibrium, in fact, only about $^2/_3$ of equilibrium coverage is reached at t_b, when the H_2O dipoles experience a net zero orienting field. Dodecanoate adsorption continues until $t \approx 4000$ s, together with a substantial increase of the response at 3150 cm^{-1} . This response arises from water molecules oriented *opposite* to the water molecules responsible for the 3150 cm^{-1} signal at $t < t_b$, evidenced by the relative phases of adsorbate and water bands in the 2600− 3800 cm^{-1} wavenumber range (Figures 2, 3). Most likely, the hydrophobic interaction between the surfactant alkyl chains is the driving force behind dodecanoate adsorption past the point of electrostatic equilibrium.[63] In other words, the energetic advantage of re-establishing an ordered water structure near the overcharged interface to avoid numerous water−alkyl contacts at partial monolayer coverage compensates for the electrostatically unfavorable incorporation of anionic surfactant molecules into the then negatively charged adsorbate layer.

4.4. Synchronism of the Adsorption Process. It has been argued in the literature[65,66] that surface adsorption can be modeled as a multistep process, incorporating, first, the diffusion of surfactant to the interface, second, the actual adsorption at the interface, and third, the reconformation of the adsorbed molecules, that is, of their alkyl chain. The last step is assumed to be an irreversible process and very slow.[14,65]

Similar stepwise adsorption mechanisms have often been proposed; however, the time constants of the individual events are experimentally very difficult to assess. Castro et al.[67] used second harmonic generation to study adsorption phenomena and found that at the air–water interface, organic molecules (not necessarily surfactants) reach their equilibrium orientation very rapidly (in less than a fraction of a millisecond). It has already been pointed out that VSFS can probe different parts of a molecule independently and that only molecular subgroups of nonrandom orientation contribute to the resonant second-order interface susceptibility, which is essential for the generation of any sum-frequency signal apart from background. In the present experiment, we monitored the adsorption of the carboxylate headgroup and, virtually simultaneously, the signal of the methyl terminus of the dedecanoate molecule. Given the high conformational degree of freedom of the surfactant alkyl moiety, any slow ordering process of the alkyl chain would show up in a lack of correlation between the carboxylate and methyl response, because headgroup orientation should be largely determined by the constrains of the solid–liquid boundary. To cope with interference effects between OH modes of interfacial water molecules located in the 2600–3800 cm^{-1} region and the νCH_3 resonance (~2874 cm^{-1}), the νCD_3 resonance of methyl-deuterated dodecanoate (C12-D) at ~2078 cm^{-1} was used instead. The latter band is located in a region without any additional signals which would only complicate data analysis. Figure 5a shows the total nonlinear susceptibilities $\chi^{(2)}$ at the νCO and νCD_3 frequencies. Data were measured at a uniform rate of 0.06 s^{-1}, alternating the frequencies. Thus the νCO and νCD_3 are offset by a constant time interval. To determine coincident $\chi^{(2)}$ values, the raw data of the νCO signal were interpolated to the time-of-measurement of the νCD_3 resonance by averaging adjacent measurement. Data were then normalized and correlated (Figure 5b). No significant time lag between the appearance of the ν CO and νCD_3 signal can be found. The slight deviation from a linear relationship is within reasonable error limits of the procedure, and the adsorption seems to take place in a single step: both the carboxylate headgroup and the methyl terminus simultaneously transform into a well-ordered state, and—at least for laureate adsorption at the fluorite−water interface—no slow conformational alignment process of the alkyl chain can be detected.

4.5. Conformational Order of the Adsorbate Layer. The vectorial properties of the hyperpolarizabilities of molecular subunits like methylene groups can be used for an estimation

(66) Zawadzki, M. E.; Harel, Y.; Adamson, A. W. *Langmuir* **1987**, *3*, 363–368.
(67) Castro, A.; Ong, S.; Eisenthal, K. B. *Chem. Phys. Lett.* **1989**, *163*, 412–416.

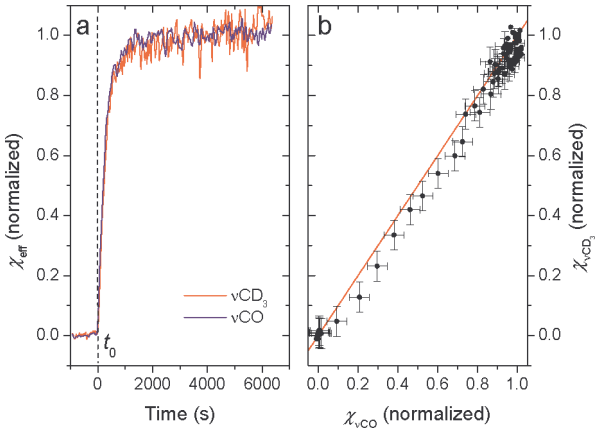

Figure 5. Temporal profile (a) and correlation (b) of the normalized nonlinear susceptibility of the νCO and νCD$_3$ bands. Red line (b) indicates perfect correlation. At t_0, C12-D concentration was increased from 0 to 30 μM, while keeping the ionic strength constant (I = 0.1 M, NaCl). Error bars are 5%.

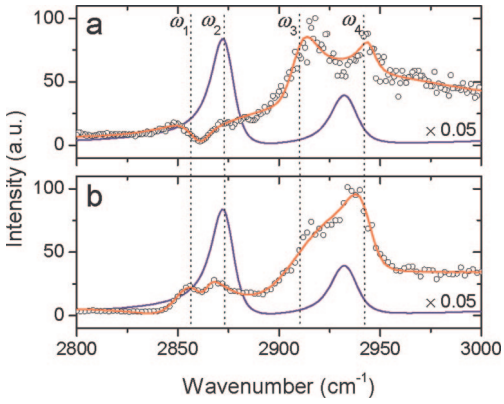

Figure 6. VSFS spectra of sodium dodecanoate at the fluorite−water interface (full monolayer coverage): (a) fully CD$_3$ deuterated surfactant (~99.8% deuteration); (b) VSFS spectra of a monolayer containing small amounts of nondeuterated dodecanoate. The blue line represents the VSFS response of a neat nondeuterated (CH$_3$) sodium dodecanoate monolayer, scaled by 0.05 (fit only). Positions of individual modes are indicated by dotted lines: ω_1 νCH$_2$ symmetrical stretch; ω_2 νCH$_3$ symmetrical stretch; ω_3/ω_4 overtones of CH$_2$/CH$_3$ deformation modes, enhanced by Fermi resonance.

of conformational order within an adsorbate layer. Becraft et al.[23] have shown that stearate forms well-ordered, tightly packed monolayers on fluorite. From the absence of any CH$_2$ response, these investigators concluded an all-trans alignment of the surfactant backbone, in agreement with findings by others.[68] This was further backed by experiments on surfactant monolayers of dodecanoate-12,12,12-d_3 on fluorite, which also play an important role for kinetic experiments of equilibrium monolayers.[39] The deuterated surfactant lacks the response from CH$_3$ groups in the 2600−3000 cm^{-1} region of the VSFS spectrum, and thus even minor signals from CH$_2$ resonances can be detected. Figure 6 shows representative spectra, obtained from a fully deuterated monolayer (Figure 6a) and a monolayer containing a small amount of hydrogenated surfactant, Figure 6b. By spectral fit, the CH$_2$ symmetric stretch can be located at ~2853 cm^{-1}, which is largely obscured in the spectrum of a hydrogenated monolayer by the CH$_3$ resonance at ~2874 cm^{-1}. Further peaks above 2900 cm^{-1} can be attributed to either the CH$_2$ asymmetric stretch mode and/or overtones of CH$_2$/CH$_3$ bending modes, the latter enhanced by Fermi resonance, but are not of particular relevance for this study. The vast difference in amplitude of the CH$_2$ and CH$_3$ modes however indicates trans alignment of the surfactant's alkyl chain for adsorbed dodecanoate, similar to its C$_{18}$ homologue,[23] stearic acid. For the latter, evidence for uncoupled OH oscillators, which are typical for smooth hydrophobic interfaces, was found at ~3650–3700 cm^{-1}.[69] The absence of this band for dodecanoate (and also for decanoate and hexanoate[23]) shows that the alkyl−water transition is less abrupt for these adsorbates compared to stearate, that is, dodecanoate monolayers are characterized by a less distinct alkyl−water boundary and/or less dense packing than stearate. Therefore, water molecules can penetrate the adsorbed dodecanoate chains to some extent and further disrupt the monolayer.

4.6. Monomer Exchange at Equilibrium: Reversibility of the Adsorbate–Substrate Interaction. The reversibility of carboxylate adsorbate layer formation at the mineral−water interface has been classified as irreversible on fluorite[11] and reversible,[10] on an alumina surface. Both studies rely on flushing procedures, i.e., water was substituted for the surfactant solution in contact with the sample. Subsequently, the adsorption density was monitored by suitable in situ IR techniques. Couzis and Gulari[10] argue that surfactant ions which are chemically bonded to surface sites are reversibly adsorbed, while electrostatic adsorption is irreversible. On the contrary, Free and Miller[11] attributed the stability of self-assembled surfactant monolayers against rinsing with neat water to chemisorption (i.e., the formation of covalent bonds between adsorbate molecules and discrete substrate sites[70]). This kind of reasoning, which relates the reversibility of monomer adsorption at the solid–liquid interface to the nature of substrate–adsorbate bonding seems to be widely accepted. For small molecules showing negligible adsorbate–adsorbate interactions.[31,32] such an approach appears straightforward, but for surfactant self-assembly on solids it has long been known that hydrophobic interactions between the alkyl chains are a major driving force,[70] evidenced by the existence of a critical concentration, the CHMC.[52] The criticality of the adsorption phenomena also raises doubts if it is valid to describe adsorption under these conditions by Langmuirian site-adsorbate interaction models despite their often excellent ability to fit experimental data.[11] Such models imply the adsorption of isolated molecules at the interface by a substrate–adsorbate complex, but the generally accepted picture for surfactant adsorption involves the formation and growth of surface aggregates, where the individual monomers are not necessarily bonded to discrete surface sites.[55] Additionally, before and after a criticality threshold, systems typically show rather different thermodynamic, transport, and kinetic properties. In particular, the kinetics of monomer exchange of an adsorbed layer and a bulk solution might be largely different for a fully established equilibrium monolayer, compared to the same monolayer under nonequilibrium conditions, or at lower than optimal local surface coverage. Desorption experiments which require nonequilibrium conditions to study equilibrium exchange kinetics therefore cannot be conclusive, at least when critical adsorption phenomena are considered.

A first account of monomer exchange at equilibrium monolayers has already been presented in a recent communication.[39]

(68) Jang, W.-H.; Miller, J. D. *J. Phys. Chem.* **1995**, *99*, 10272–10279.

(69) Brown, M. G.; Walker, D. S.; Raymond, E. A.; Richmond, G. L. *J. Phys. Chem. B* **2003**, *107*, 237–244.

(70) Fuerstenau, D. W. *Pure Appl. Chem.* **1970**, *24*, 135–164.

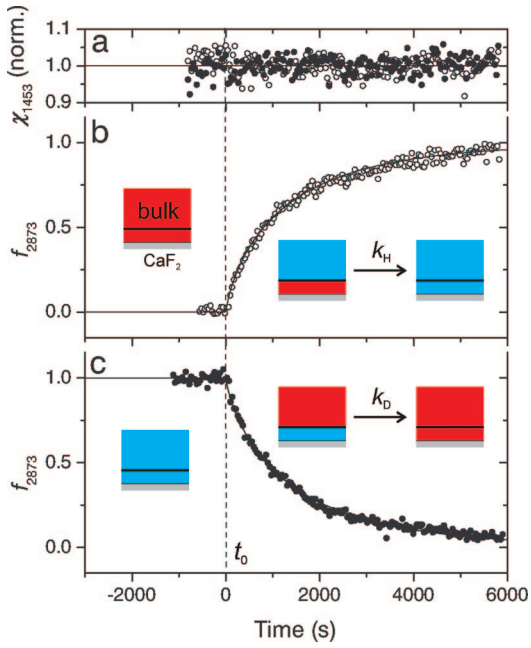

Figure 7. Monomer exchange kinetics of sodium dodecanoate at the fluorite−water interface (circles, fully deuterated monolayer for $t < t_0$; bullets, fully hydrogenated monolayer for $t < t_0$):[39] (a) normalized nonlinear optical resonse of the carboxylate headgroup; (b) exchange kinetics (k_H) of a deuterated monolayer and (c) of a hydrogenated monolayer (k_D). At t_0, the bulk liquid phase was replaced by a hydrogenated (b) or a deuterated surfactant solution (c) of equal concentration (10 μM). The exchange process was then followed by the sum-frequency signal at 2873 cm^{-1}, corresponding to the CH_3 symmetrical stretch; f_{2973} is the mole fraction of hydrogenated surfactant in the monolayer.[39] In the pictorial representation, blue areas correspond to hydrogenated, red areas to deuterated surfactant molecules. The gray slab represents the CaF_2 substrate; the black line is the boundary between monolayer and bulk.

In short, this study used an experimental scheme based on a sudden change of the bulk composition from hydrogenated to deuterated surfactant,[7,71] or the reverse. During this change, the response of the surfactant's CH_3 terminus was monitored, and related to the mole fraction of hydrogenated surfactant in the monolayer, f_{2873}.[39] In analogy, the CD_3 signal can be used to determine the amount of deuterated surfactant in the monolayer. Note that throughout the experiment, the adsorption density of surfactant molecules regardless of their isotopic composition can be monitored by the nonlinear susceptibility of the carboxylate headgroup response.[39]

Figure 7 shows typical results for a self-assembled sodium dodecanoate monolayer, quasi-simultaneously recording the sum-frequency signals of the carboxylate headgroup (1453 cm^{-1}) and of the methyl terminus, at 2873 cm^{-1}. Two experiments are presented: one starting with a fully deuterated monolayer (Figure 7b), the other starting with a fully hydrogenated monolayer (Figure 7c). From the constant headgroup response at 1453 cm^{-1} (Figure 7a) we can directly infer equilibrium adsorption in both cases. In the case of the initially deuterated monolayer (Figure 7b), the bulk surfactant solution was, at time t_0, replaced by a solution of identical concentration, but containing hydrogenated dodecanoate only. Immediately, the sum-frequency signal at 2873 cm^{-1} (νCH_3) increases, because hydrogenated surfactant is incorporated into the (previously, at 2873 cm^{-1}, not sum-frequency active) monolayer. The

(71) Khan, A.; Ducker, W. A.; Mao, M. *J. Phys. Chem. B* **2006**, *110*, 23365–23372.

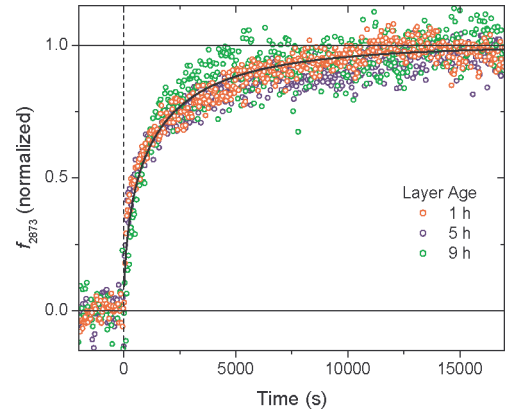

Figure 8. Monomer exchange kinetics of sodium dodecanoate at the fluorite−water interface. Monolayers generated in situ from surfactant with CD_3 terminus were aged for 1 to 9 h. At t_0, hydrogenated dodecanoate was introduced. The exchange process was followed by the sum-frequency signal at 2873 cm^{-1} (CH_3 symmetrical stretch) and is given as mole fraction of hydrogenated surfactant in the monolayer, f_{2873}.

fraction of hydrogenated molecules can be directly derived from the 2873 cm^{-1} second-order susceptibility,[39] and the rate of monomer exchange k_H can so be obtained from the time-dependent data. The reverse reaction, which starts with a full hydrogenated monolayer (Figure 7b) can be treated analogously and results in virtually identical kinetics characterized by a rate constant k_d. Using a simplified model of the exchange mechanism,[39] we concluded from the equality $k_D \approx k_H$ that the incorporation of a molecule into the monolayer as part of the exchange process is followed by very rapid conformational alignment of the alkyl chain. This finding is now additionally supported by the absence of a slow conformational alignment period during adsorption discussed before.

Further exchange measurements were performed on monolayers of different age, but otherwise grown under very similar conditions. Again, the νCH_3 response at 2873 cm^{-1} was used to follow the exchange process (Figure 8). Aging of adsorbate layers presents an easy means of studying correlations between exchange kinetics and defect concentrations. It seems intuitive and will be demonstrated by desorption experiments below that the fairly rapidly grown monolayers initially contain a number of defects, which are, at least partly, cured over the course of hours. Despite some inevitable variation of the data caused by instrument drift over the long observation times and arguably slightly different properties of the fluorite surface (polishing, roughness induced by partial dissolution of the semisoluble salt), the traces are remarkably similar (Figure 8); interestingly, the age of the monolayer has little effect on monomer exchange kinetics. This is in agreement with the proposed exchange mechanism, whereby the monomer release is spontaneous and the time-determining step.[39] Experiments performed at different bulk surfactant concentrations (10 or 30 μM) were used to show that a higher rate of collisions between bulk surfactant molecules and the monolayer, which would occur at higher concentrations, does not significantly affect the process.[39] Therefore, the monomer exchange rate can be considered an intrinsic property of the monolayer, and, accordingly, molecular exchange reactions are not a phenomenon only occurring at surface defects or other discontinuities. Collisions between (monomeric) bulk surfactant molecules and the interfacial layer do not initiate the monomer exchange reaction.

The rate constant of the monomer exchange reaction at sodium dodecanoate monolayers ($\sim 8 \times 10^{-4}$ s^{-1}) determined

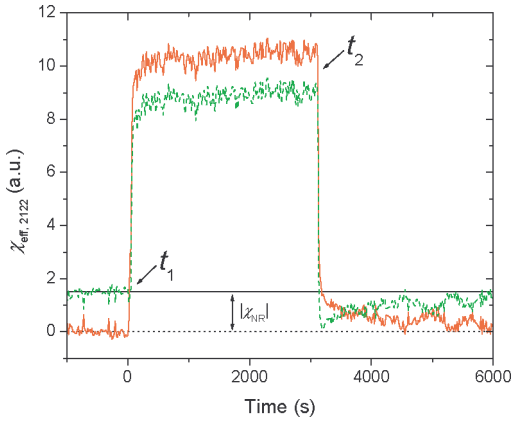

Figure 9. Monomer exchange kinetics of sodium acetate (0.333 M, pH 5.95) at the fluorite-water interface. The prism was first exposed to hydrogenated acetate. At t_1, deuterated acetate was introduced and flushed out again by hydrogenated acetate at t_2 . The green curve shows the total effective susceptibility at 2122 cm^{-1}, which was corrected for the (destructively interfering) nonresonant background χ_{NR} to yield the resonant contribution attributable to the CD_3 group (red curve).

in this and an earlier VSFS study[39] is significantly smaller than related exchange rates of surface-adsorbed micelles (on the order of 1 s^{-1}),[7] which are largely lacking direct substrate-headgroup contacts. This poses the question, if the much slower rate observed in the present case can be attributed to headgroup bonding at the fluorite surface. To elucidate this point, experiments with hydrogenated and deuterated acetate ions were performed. Acetate does not show critical adsorption behavior, nor does charge reversal of the interface occur, even at high concentrations.[32] Adsorption is thus unlikely to be affected by hydrophobic or any other cooperative effects. The chemical properties of the acetate carboxylate group, however, should be very similar the those of the dodecanoate headgroup. Figure 9 shows the CD_3 response of a fluorite−water interface during a change from hydrogenated to deuterated acetate, and back, while all other parameters were left unchanged. The data clearly indicates that, compared to adsorbed dodecanoate, the exchange of surface-adsorbed acetate is faster by orders of magnitude: in less than 45 s, over 90% of the VSFS-active molecules are replaced. The exchange reaction is far too fast to allow for a meaningful determination of a rate constant, given the temporal resolution of the present instrument (0.06 s^{-1}).

These findings for acetate, combined with the observations of dodecanoate monolayers lead to the conclusion that the headgroup-substrate interaction only plays a minor role for monomer exchange kinetics and thus, the reversibility of the adsorbate bonding. The energy barrier governing the rate constant of monomer release appears to be determined by other factors, such as the energetic cost of transferring a monolayer-bonded molecule into a monomeric bulk state, therefore generating an unfavorable hydration structure around the alkyl moiety. Bulk or substrate-bound micelles can more easily tolerate the release of single monomers due to their highly flexible nature, where a transient change in the aggregation number can be easily compensated by slightly altering their geometrical shape, without exposing any hydrophobic moieties to water at the micellar surface. For monolayers at the solid–liquid interface, the geometry and total interfacial area is invariably determined by the substrate, thus increasing the energy barrier of monomer release.

4.7. Effects of Surface Coverage and Aging on Desorption Kinetics. The general picture of monolayer desorption has already been discussed in an earlier communication.[39] Briefly, the structure of the water layer adjacent to the interface is severely disturbed upon substitution of the bulk surfactant solution by water, despite the virtually unchanged coverage of the surface. It has further been found that monomer release from a monolayer in contact with neat water, that is, in a nonequilibrium state which finally leads to desorption, is much slower compared to an equilibrium monolayer and characterized by a substantial induction time. The latter was tentatively attributed to the difficulties of removing more than a few monomers of a complete monolayer at a time, which would cause energetically unfavorable contacts of water molecules with surfactant alkyl chains. However, even under such conditions, small amounts of dodecanoate are eventually removed and their concentration in the bulk is kept near zero by constant flushing of the fluorite surface with neat water. Once a certain critical level of monolayer defects (critical surface density) is reached, the rate of desorption increases rapidly and proceeds with near-exponential kinetics.

It was found that a good empirical description of the nonlinear susceptibility during desorption can be obtained by a decay function derived from Weibull statistics, followed by a monoexponential decay. The Weibull distribution is one of the most widely used lifetime distribution models.[72] In the present case, the release of a surfactant molecule is considered the elementary statistical event. This model is fairly flexible and allows, in particular, the description of induction phenomena. In eq 5, a time t' is used to distinguish the Weibull and exponential desorption regime:

$$A(t) = \begin{cases} A_\infty + (A_0 - A_\infty)\exp\{-(t/\lambda)^k\}, & t \le t' \\ A_\infty + (A_0 - A_\infty)\exp\{-(t'/\lambda)^{(k-1)}[t(k/\lambda) + t'(1-k)/\lambda]\}, & t > t' \end{cases} \quad (5)$$

Amplitude A_0 is found at $t = 0$, the time when flushing with neat water commences. A_∞ is the residual (nonresonant) amplitude after desorption of the monolayer; k is the shape parameter of the Weibull distribution ($k > 0$). For $k = 1$, Weibull and exponential distributions are identical. The scale parameter λ is related to the typical lifetime of a monolayer at the surface after transition of the monolayer into its nonequilibrium desorption state.

Figure 10a shows experimental data for desorption experiments, which were fit by eq 5. The original layers differed in age and surface coverage. Interestingly, $k = 1.2$ (near exponential desorption) was found when starting from incomplete coverage (green curve, Figure 10), while values of $k \approx 3.2-4.2$ were observed for desorption of layers which were complete prior to flushing with neat water. The effect of monolayer age on desorption kinetics is notable. It was also found that to some degree, surface roughness affects desorption kinetics, because monolayers on freshly polished substrates seem to have exhibited somewhat slower desorption kinetics. A detailed investigation, however, is made difficult, because the initial surface properties are not as easily controllable as monolayer age. Frequent polishing of the CaF_2 substrate was employed to perform experiments under reproducible conditions, but the observations nevertheless point out the importance of monolayer defects for desorption.

(72) Lawless, J. F. *Statistical Models and Methods for Lifetime Data*; Wiley-Interscience: Hoboken, NJ, 2003.

From fits, estimates for typical scale parameters, λ, were determined and ranged from ~1500 s for incomplete layers to $4.8 \pm 0.8 \times 10^3$ s for the desorption of fully established monolayers. These considerable differences in the desorption rates corroborate the notion that desorption commences at surface defects, which can either be already present in the monolayer of generated by spontaneous release of single monomer molecules. As long as coverage is incomplete, there will be numerous defects and boundaries which facilitate desorption. Such gaps are closed shortly before full coverage is reached. This final step, although only accompanied by a minor increase in surface coverage, can thus render the kinetics of monolayer's dynamics distinctively different. To further investigate this aspect, experiments were performed on a monolayer grown to practically full coverage, but using a bulk surfactant solution just above the CHMC. Under these conditions, final equilibrium is very slowly established, as the driving force of the adsorption (i.e., the difference between bulk concentration and CHMC) is small. Thus, desorption can be conveniently initiated before the monolayer reaches its true equilibrium state (red curve, Figure 10). From the fit, a value of $k \approx 2$ was obtained ($\lambda \approx 3.2 \times 10^3$ s). Therefore, a major increase of k in the region of almost full surface coverage can be inferred, that is, the initially very slow desorption which is apparent as an induction time is a property of only the complete and equilibrated monolayer.

The instantaneous rate of monomer release $d(t)$, which links the number of released monomers per time step to their total number left on the surface, can be deduced from eq 6:

$$d(t) = \lim_{\Delta t \to 0} \frac{A(t) - A(t+\Delta t)}{\Delta t[A(t) - A_\infty]} = \begin{cases} \frac{k}{\lambda}\left(\frac{t}{\lambda}\right)^{k-1}, & t \le t' \\ \frac{k}{\lambda}\left(\frac{t'}{\lambda}\right)^{k-1}, & t > t' \end{cases} \quad (6)$$

Note that $d(t)$ is constant for exponential kinetics ($t > t'$), but increases over time for Weibull distributions with $k > 1$, and decreases for $k < 1$, at $t \le t'$. Figure 10 parts b and c show a comparison of desorption rates calculated from the fits and numerically from the raw data. Good agreement was found even for this derived quantity. Only at $t > 5000$ s, does the change of the signal per unit time become too small to allow for a meaningful numerical analysis. For $t < 5000$ s, the data clearly reveal that the rate of the desorption reaction is far from constant, in contrast to common simplified models, which focus on individual adsorbate–substrate contacts rather than the growth of surface aggregates during the adsorption process, driven by hydrophobic interactions.[11,55] Interestingly, at low coverage, the desorption rate attains a value ($\sim 1 \times 10^{-3}$ s^{-1}) similar to equilibrium monomer exchange,[39] which appears somewhat intuitive as the advantage of an at least partly intact monolayer then vanishes.

From these results we conclude that surface defects introduced by the physical structure of the substrate can significantly affect interfacial kinetics. This has to be considered in particular, when kinetic data of studies performed on highly flat, monocrystalline substrates are compared with results obtained using powdered or microcrystalline solids.

4.8. Electrolyte Effects on Kinetics at the Solid–Liquid Interface. Many adsorption processes of practical relevance take place in solutions containing appreciable concentrations of electrolytes, and the presence of ions will greatly affect the structure of the solid–liquid interface and therefore alter kinetics of interfacial processes.[11] Under the conditions of this study, the fluorite surface is positively charged, thus sodium salts of two commonly encountered anions, chloride and sulfate, were chosen for this investigation. So far, no VSFS spectra of these electrolyte solutions at the fluorite−water interface have been reported and were therefore determined first. Figure 11 shows data for a representative set of concentrations, corresponding to an ionic strength of up to 0.1 M. While a more detailed analysis of these and other electrolytes at the CaF_2 interface will be presented elsewhere, we only want to focus on the more general features relevant for this study. The differences between chloride (Figure 11a) and sulfate (Figure 11b) are striking: at $I = 0.01$ (blue curves), chloride only has a small effect on the population of interfacial water molecules and their bonding environment, while a severe decrease of intensity is observed for sulfate. Additionally, at the higher sulfate concentrations, the water bands at ~3200 and ~3450 cm^{-1} are not only

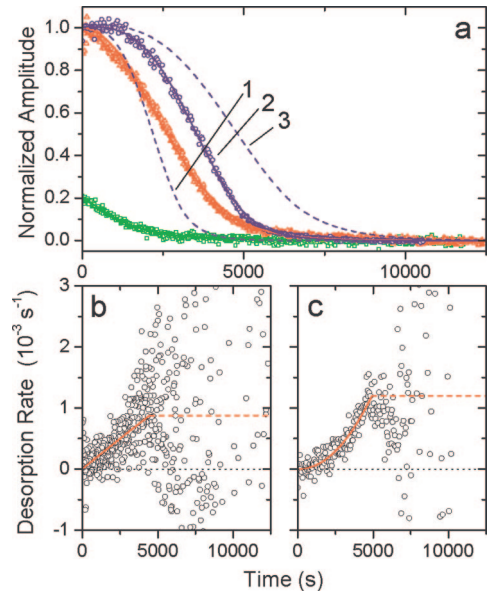

Figure 10. Desorption kinetics of sodium dodecanoate at the fluorite−water interface. (a) Data obtained for monolayers of different initial coverage and age: incomplete coverage (green), nonequilibrated layer close to full coverage (red, curve R), and equilibrated, complete layers of varying age (blue, curves B; (1) 1 h, (2) 2 h, and (3) 12 h). Panels b and c show instantaneous desorption rates for curves R and B (2 h), respectively, and were derived numerically (circles) or from the fits (red curves).

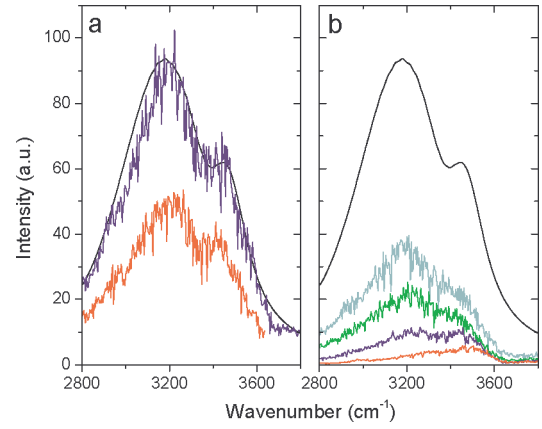

Figure 11. VSFS spectra of the CaF_2 (aq) interface in the presence of sodium chloride (a) or sodium sulfate (b) solutions. The black solid curve represents the response of the neat CaF_2−water interface. Ionic strength (in M): (a) $I = 0.01$ (blue), $I = 0.1$ (red); (b) 0.0001 (light blue), 0.001 (green), 0.01 (blue), 0.1 (red).

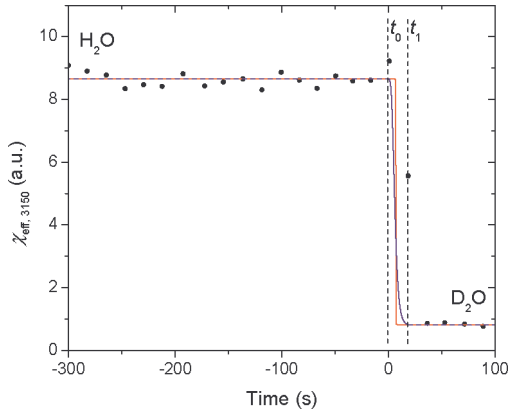

Figure 12. H_2O/D_2O exchange at the neat fluorite−water interface. D_2O was introduced into the cell after finishing collection of the datapoint (at t_0) by rapid flushing, and exchange of the bulk phase can be considered complete sometime before t_1. Values shown are averages of the effective nonlinear susceptiblity at 3150 cm^{-1} over 15 s intervals. Red and blue curves shows possible transition kinetics (extremal cases).

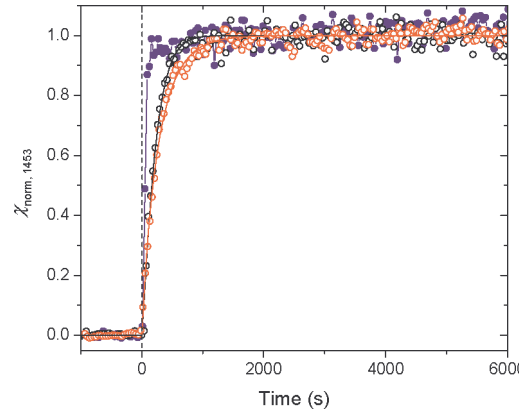

Figure 13. Adsorption kinetics of C12-H (30 μM) at the fluorite−water interface in the presence of sodium chloride. Red and black circles show typical experimental data at $I = 0.1$, curves are monoexponential fits. Data represented by blue bullets/lines were obtained without added electrolyte.

diminished, but their relative population changes favor water molecules in a more disordered state, associated with the band at higher energy.

For monovalent anions, the strong hydration of fluorite has been used by Hu et al.[25] to explain the insensitivity of its electrokinetic behavior toward the bulk F^- concentration, and FTIR-IRS experiments by the same investigators revealed a unique hydration state of the CaF_2 surface. A strong orientation of water molecules and a high degree of structuring in the water layer adjacent to this substrate was also observed in an earlier VSFS study.[21]

An appreciable quantity of oriented water present at the interface even at a chloride ionic strength $I = 0.1$ raises questions concerning the dynamism of the water−fluorite interaction: is there a stagnant, strongly bound hydration layer at the interface, which can only be replaced by highly negatively charged anions or other molecules showing a strong calcium-adsorbate interaction, or is this water layer in dynamic equilibrium with the bulk? Using isotopic labeling similar to the method described above, experiments on the H_2O/D_2O exchange at the fluorite−water interface were performed (Figure 12). Our VSFS data reveal that the H/D exchange is rapid, and the nonlinear susceptibility of the interface reaches its nonresonant background value within an interval of less than ∼15 s, the temporal resolution of the present apparatus. This provides evidence for a highly dynamic interfacial water layer, and even though this layer persists up to high chloride concentrations, constant exchange between bulk and surface-coordinated water molecules or at least protons is observed. For chloride anions, the electrical double layer appears to be purely diffuse, that is, no dense layer of counterions is formed at the interface. Only the stronger Coulombic interaction of divalent ions (sulfate) with the positively charged fluorite can compensate for the decrease in hydrogen-bonding energy when water molecules are displaced from the CaF_2 surface, and occupy sites directly at the solid–liquid boundary. Note that even at the highest sulfate concentration studied ($I = 0.1$) interfacial water molecules still experience a positive surface charge (as evidenced by the phase of the OH bands) and therefore the adsorption of sulfate ions does not lead to overcharging of the substrate.

4.8.1. Effects on Adsorption Kinetics. It has just been demonstrated that ions, in particular sulfate, significantly alter the structure at the solid–liquid interface. Electrolytes are also expected to interfere with the adsorption process: on one hand, they screen the charge of the (positively charged) fluorite substrate and of (ionic) adsorbates. On the other, ions may compete for surface sites with surfactant molecules, thus rendering adsorption unfavorable, at least at low coverage, when electrostatics are the predominant driving force.[15]

For this study, adsorption experiments were performed in sodium chloride ($I = 0.1$) and sodium sulfate solutions ($I = 0.001$, $I = 0.01$). A surfactant concentration of 30 μM was chosen for all experiments, to avoid artifacts arising from any transport limitation. Figure 13 shows the results obtained in the presence of chloride anions. From this data, we conclude that the interaction of chloride ions with the interface leads to a smaller adsorption rate, but their effect even at high concentration is small. Furthermore, within the experimental error (∼3%), adsorption reaches the same coverage as in the absence of electrolyte. From fits of the data with monoexponential kinetics, a reduction of the rate of adsorption by a factor of ∼5 was found ($4.0 \pm 0.4 \times 10^{-3}$ s^{-1} at $I = 0.1$, compared to $2.2 \pm 0.5 \times 10^{-2}$ s^{-1} at $I = 0$). Additional experiments showed that the rates at $I = 0.01$ and $I = 0.1$ of chloride are similar. Note that for cationic surfactants, an increase of the adsorption rate was found on a positively charged silica−water interface and attributed to electrostatic screening.[14] For the adsorption of an anionic surfactant (e.g., of C12-H) on a positively charged solid, electrostatic screening causes a decrease of attractive forces between adsorbate and substrate which naturally results in a *smaller* rate of adsorption.

Electrostatic screening, however, does not appear to be the only reason for the slowing-down of adsorption kinetics. Screening should predominantly depend on ionic strength rather than on the specific nature of the electrolyte, but in the presence of sulfate the timescales of adsorption are completely changed (Figure 14). Additionally, the equilibrium adsorption, even at $I = 0.001$, does not reach full coverage. At $I = 0.01$ no noticeable adsorption could be observed within several hours. Obviously, surfactant monomers and sulfate ions compete for adsorption sites, and the energetic gain arising from the interaction of the surfactant molecules' alkyl chains is not high enough to fully compensate the Coulombic fluorite−sulfate bonding. Furthermore, the initial rate of adsorption in the presence of sulfate is very low, especially for a freshly polished

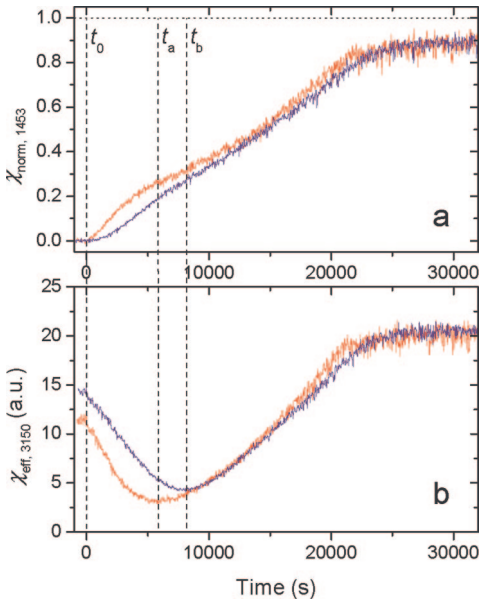

Figure 14. Adsorption kinetics of C12-H at the fluorite−water interface (blue, freshly polished; red, etched) in the presence of sulfate: (a) carboxylate headgroup signal (1453 cm^{-1}); (b) amplitude attributed to interfacial water molecules (3150 cm^{-1}). At t_0, neat electrolyte solution ($I = 10^{-3}$ mol L^{-1}; Na_2SO_4) was replaced by a 30 μM C12-H (aq; $I = 10^{-3}$ mol L^{-1}; Na_2SO_4). Charge neutrality is reached at t_a (red curve) or t_b (blue curve).

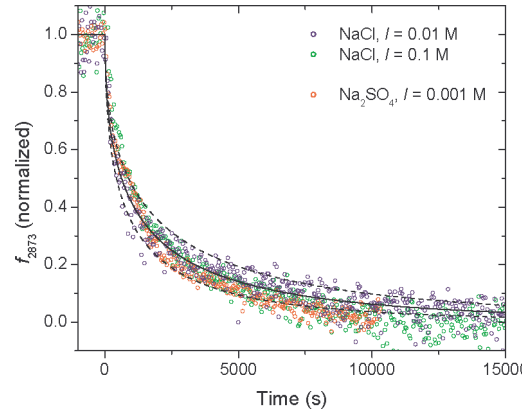

Figure 15. Comparison of the temporal profile of the corrected sum-frequency reponse at 2873 cm^{-1} (f_{2873})[39] for the exchange reaction of a fully hydrogenated monolayer by C12-D. The aqueous phase contained NaCl or Na_2SO_4 at different ionic strength, I . Range of experimental data without added electrolyte are indicated by dashed curves, the black solid curve represents the average.

substrate. Only after an induction time of the order of 1000 s, does formation of a monolayer commence. This indicates that the generation of nucleation sites for surfactant adsorption,[15] a very rapid process in the absence of electrolyte at 30 μM surfactant concentration, is significantly hindered by the presence of sulfate ions at the interface; that is, the interaction between sulfate ions and small aggregates of (or even single) adsorbed surfactant molecules is highly unfavorable, and it takes significant time until a notable number of nucleation sites form. As in other cases of nucleation-limited kinetics, surface defects should play an important role during this initial period. Over the course of experiments, it was observed that the adsorption kinetics of C12-H in sulfate-containing solutions is affected by the state of the surface. Compared to a polished CaF_2 substrate, adsorption onto a mildly etched surface is characterized by a much shorter induction time and a higher initial rate of adsorption (Figure 14, red curve). Note also that at the point of charge neutrality of the interface with respect to the interfacial water molecules (as measured by their nonlinear susceptibility at 3150 cm^{-1}, Figure 14b), the rate of adsorption changes again. At this point, coverage amounts to approximately 25%, thus the rate should no longer be limited by nucleation. Apparently, even in a region of coverage when surface aggregation of surfactant can be considered hydrophobically driven, the sulfate ions present at the interface represent a high energetic barrier, and the shape of the adsorption curve suggests that the release of sulfate is likely to be time-determining for the reaction. The strong competition between surfactant and sulfate adsorption is also evident from the maximum coverage attainable in equilibrium, which does not exceed ~90%, compared to adsorption from neat water or chloride solutions.

4.8.2. Electrolyte Effects on Equilibrium Exchange Rates. In section 4.6 we discussed monomer exchange kinetics at a dodecanoate monolayer in the absence of electrolyte and it was concluded that monomer release is the rate-determining step.[39] It might thus be inferred that the monomer exchange rate should be rather insensitive to the presence of electrolyte in the bulk, because it is an inherent property of the monolayer and not significantly affected by the bulk surfactant concentration.

To get some further insights, a series of experiments were performed in the presence of sodium sulfate or sodium chloride. Figure 15 shows the results of these efforts. All experiments started with a fully equilibrated C12-H monolayer, which was then exposed to a C12-D solution of equal surfactant concentration (30 μM) and ionic strength (note that for Na_2SO_4, $I = 3c$). The data clearly show that within the error and scatter of the experiment, background electrolytes hardly affect the exchange kinetics of the dodecanoate monolayer at the fluorite−water interface and therefore support the proposed mechanism of the exchange process.

Despite only partial coverage being reached in the presence of sulfate (~90%), exchange dynamics are largely unchanged. We attribute this to a nonuniform distribution of surface defects caused by coadsorbed sulfate ions. The monolayer thus features larger, undisturbed regions of full coverage, interspersed with clusters of sulfate ions. Further support for this picture comes from the well-organized structure of the hydrogen-bond network adjacent to a sulfate-containing monolayer, as the only small difference in the 3150 cm^{-1} νOH signal, indicative for the degree of ordering at the monolayer (see later, Figure 16), appears to be at odds with a relatively high defect concentration of 10%, if these defects were uniformly distributed across the surface.

4.8.3. Effects on Desorption Kinetics. Surprisingly little is known about the effect of electrolytes on desorption kinetics of adsorbate layers at the mineral-water interface, although it is well-established that ionic strength and the specific nature of a salt can affect adsorption kinetics, equilibrium adsorption density, or both.[11,14,73] Desorption data are largely missing, but would be essential for various fields, for example, processes relying on the transport of organic substances by means of adsorption/desorption steps in chromatography, in the environment, and in numerous technical applications that involve recovery or removal of adsorbed surface-active agents from substrates in the presence of salts.

(73) Gomari, K. A. R.; Hamouda, A. A.; Denoyel, R. *Colloids Surf. A* **2006**, *287*, 29–35.

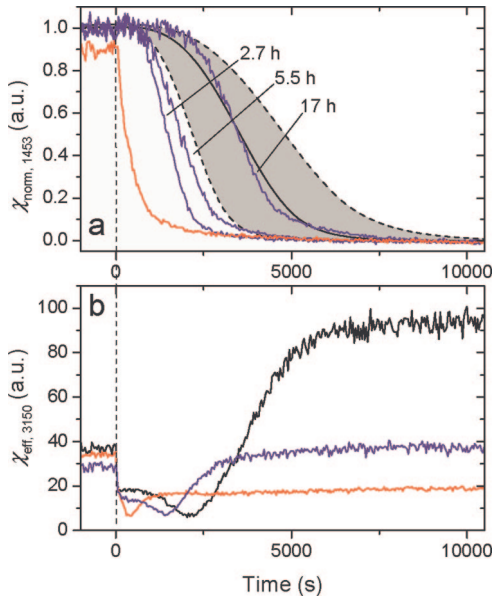

Figure 16. Desorption kinetics of dodecanoate monolayers at the fluorite−water interface: (a) typical data of the νCO response (1453 cm^{-1}) during desorption in the presence of sodium chloride (blue, $I = 0.1$, age of layer is also shown) or sodium sulfate (red, $I = 0.001$). Gray area and black dotted and solid curves show data without added electrolyte; (b) response of interfacial water molecules at 3150 cm^{-1} (black, $I = 0$;[39] blue, NaCl, $I = 0.1$, 5.5 h; red, Na_2SO_4, $I = 0.001$).

Considering the number of relevant electrolytes and adsorbates, nonlinear optical techniques open a wide field of research in this area, and this part of the present study merely is a proof-of-principle using sodium dodecanoate monolayers as an exemplary adsorbate layer. The experimental protocol was virtually identical to the studies in the absence of background electrolyte (section 4.7), except that NaCl or Na_2SO_4 was added to adjust the ionic strength of the bulk medium. Some results are presented in Figure 16.

Figure 16a shows the susceptibility arising from the resonant response of the surfactant headgroup. Clearly, the presence of chloride ions somewhat accelerates the desorption process, and aging of the monolayer incurs similar effects. In particular, a notable induction period was observed. This indicates that even at $I = 0.1$ of NaCl, a complete monolayer is formed, with desorption characteristics resembling those found in the absence of electrolyte, because the chloride does not strongly adsorb to the fluorite surface.[32]

In the presence of sulfate, desorption follows strikingly different kinetics, even at very low ionic strength ($I = 0.001$). Starting from below full-monolayer coverage, surfactant is rapidly released. The desorption rate was estimated from an exponential fit of the data ($k = 1$, eq 5), and $\lambda \approx 5.5 \times 10^2$ s was obtained. This time constant is considerably smaller compared to the related value of an incomplete monolayer (1500 s). Thus, sulfate ions not only occupy surface sites which preclude the formation of a complete monolayer, but their strong coordination to the fluorite surface also considerably accelerates the desorption process. This is in-line with the observation of other investigators, which found the sulfate solutions can quite efficiently displace adsorbed carboxylates from calcite substrates.[73]

Using VSFS, not only monolayer properties can be measured, but the orientation and magnitude of interfacial water structuring can be probed as well.[39] Figure 16b shows typical traces of the second-order susceptibility at 3150 cm^{-1} arising from interfacial water molecules in a highly coordinated state.[21] Before water is introduced into the sample cell, surprisingly similar amplitudes of the interfacial water response were observed. Consequently, the (then) negatively charged interface counteracts any specific anion adsorption at the monolayer−water boundary, and sodium ions do interfere much with the interfacial hydrogen-bonding structure. The amplitude in the presence of NaCl ($I = 0.1$) is the lowest, but this may not necessarily be because of a concentration enhancement at the surface, as even the bulk solution contains a considerable amount of sodium and chloride ions at such high ionic strength that their presence near the interface is inevitable.

After switching the solution flushing the prism surface from surfactant solution to neat water or electrolyte solutions, the same rapid decrease of water intensity if observed as discussed before.[39] Using these experiments, we conclude that this effect is not due to the change of ionic strength occurring in the absence of electrolyte when the surfactant concentration is changed, or to any other single-ion electrostatic phenomenon, but that it is directly linked to the structure of the interface between the (hydrophobic) alkyl chains of the adsorbed surfactant and the adjacent water layer.

With continuing desorption, parts of the fluorite surface are exposed to the bulk liquid and water structuring directly at the fluorite substrate commences again (Figure 16). Finally, the second-order susceptibilities at 3150 cm^{-1} reach plateau values similar to the neat fluorite-electrolyte solution interface after desorption is complete.

5. Conclusions

This study focuses on the temporal evolution of the monolayer−water interface. We use VSFS, as a nonlinear optical technique, to investigate the adsorption, desorption, and equilibrium exchange mechanisms and to determine quantitative kinetic parameters. The neat fluorite−water interface shows sum-frequency response characteristics of highly structured water in the interfacial region. This structure is severely disrupted immediately upon the introduction of surfactant into the flow cell, even though the monolayer growth would have barely commenced. Adsorption then proceeds and continues far beyond the point of electrostatic equilibrium, leading to a negatively charged monolayer. A flip in the water orientation at overcharged adsorbate layers was observed in our earlier studies, this time, however, we were able to continuously monitor the state of the surface by the second-order susceptibility of characteristic adsorbate and water modes. We also introduce and determine isotherms specific to *oriented* adsorption, as opposed to thermodynamic isotherms which measure the total surface excess, to characterize the formation of mesoscopically ordered surface aggregates.

Using the present in situ approach, we can also show that monomers are—on the time scale of the current experiments—incorporated into a growing monolayer by a single-step process, because adsorption of the headgroup and conformational alignment of the surfactant's highly flexible alkyl moieties were found to be simultaneous. The present observations can be explained by a nonuniform growth of the monolayer and a "patchy" structure of the interface at partial coverage, with some regions featuring nearly perfect adsorbate layers, and others with the fluorite surface directly exposed to the aqueous phase. It might be this mode of monolayer growth which is also responsible for defects initially present in the monolayer. Once virtually

complete coverage is reached, aging of the adsorbate layer cures a considerable fraction of these defects over the course of hours. While the defect concentration does not significantly affect monomer exchange kinetics, because this process takes place across the whole interface, with defective areas only being a small fraction of the total adsorbate layer, desorption kinetics strongly depend on the age of the monolayer. This can be understood from the mechanism of desorption, which involves a very slow initial release of surfactant molecules into neat water, evidenced by a considerable induction time. At high defect concentration, or starting from incomplete coverage, this process is enhanced, leading to an immediate onset of desorption.

From these observations we conclude that the actual kinetics at the solid–liquid interface are far too complicated to be adequately modeled by considering only substrate–adsorbate interactions. Cooperative effects simply must be considered, as soon as adsorbates showing considerable hydrophobicity are concerned. In particular, surface-assembled monolayers may appear irreversibly bonded to the surface when the surfactant solution is replaced by neat water, although a relatively rapid and complete exchange of surface-adsorbed molecules is observed for the monolayer in contact with its equilibrium bulk solution. Such kinetic inhibition effects are presumably even stronger for long-chain carboxylates and other adsorbates forming very dense, well-ordered layers on mineral surfaces.

We also provide the first insights by VSFS into electrolyte effects on the structure of the fluorite−water interface. Marked differences were found between (monovalent) chloride and (divalent) sulfate ions. The latter cause a dramatic slowing of adsorption and also compete with surfactant molecules for sites at the fluorite substrate, thus preventing full coverage in the presence of even minute concentrations of sulfate. Chloride ions seem to reside only in a diffuse interfacial layer. Their presence leads to a slowing of adsorption and an acceleration of desorption kinetics, which can be explained by electrostatic arguments. Interestingly, the equilibrium monomer exchange process is not significantly affected by the presence of electrolyte, thus showing that the dynamism of the monolayer is determined by hydrophobic rather than by any Coulombic effects. Additional experiments on the exchange reaction of fluorite-adsorbed acetate ions showed that the headgroup−adsorbate interaction cannot be held responsible for the observed kinetics, which show that surface bonding is reversible, but that monomer exchange is still slower by orders of magnitude compared to related processes of surface-bound micelles or bulk aggregates. We attribute this slowing-down to the geometrical constrains imposed onto the aggregate structure by the solid support, which makes the interfacial water structure much more sensitive to changes in monolayer structure compared to unsupported aggregates. Such entities can readily compensate a release of molecules by slight variation of shape, whereas only very few molecules can be withdrawn from a complete monolayer before unfavorable water−alkyl contacts appear as the monolayer breaks up.

Acknowledgment. Financial support for this work by the Department of Energy, Basic Energy Sciences, Grant DEFG02-96ER45557, and the Office of Naval Research is gratefully acknowledged. S.S. appreciates a scholarship of the German Research Foundation (DFG, Bonn). G.R. thanks the Guggenheim Foundation for support.

JA076664R